International Journal of Engineering Inventions
e-ISSN: 2278-7461, p-ISSN: 2319-6491
Volume 14, Issue 4 [April. 2025] PP: 101-105

Investigate the influence of contact angles of cooling channel on electric vehicle battery pack cooling efficiency

Nguyen Thanh Cong[1], Nguyen Thi Thuy Hang[2] Nguyen Thanh Thuy[3]
[1,2,3]Faculty of Vehicle and Energy Engineering, Thai Nguyen University of Technology, Thai Nguyen, Vietnam

ABSTRACT: *Cylindrical lithium-ion batteries have been widely used as a power source for electric and hybrid vehicles because of their compact size and high-power density. Furthermore, along with a few other parameters, the operating temperature of the battery in an electric vehicle plays a vital role in its performance. In this study, four different types of cooling channel structures using liquids (structure A, B, C, and D) with different contact angles are proposed to simulate and investigate their effects on cooling efficiency. The obtained results have shown that Structure C has better cooling effect than the other three structures.*

KEYWORDS*: Lithium-on battery, thermal model, temperature distribution, contact angles, electric vehicles.*

Date of Submission: 13-04-2025 Date of acceptance: 26-04-2025

I. INTRODUCTION

Electric vehicles (EVs) are being considered as replacements for existing fossil fuel-driven cars because they do not have emissions [1-4]. In this regard, Lithium ion (Li-ion) batteries are widely used as power sources for EVs. However, Li-ion batteries are more sensitive to operating temperature, the limited temperature of the battery pack has become the major challenge for their wide application [5]. It is well-known that the best working temperatures for Li-ion batteries are in the range of 15°C to 35°C, and the best maximum temperature difference within the battery packs is less than 5°C [6]. Therefore, a battery thermal management system (BTMS), which can maintain an optimal operating temperature range and minimize the temperature difference between battery cells for safe and efficient driving, must be developed.

The liquid cooling method is the most widely used BTMS method nowadays due to high thermal conductivity and compact size. Depending on whether the battery pack is in direct contact with the coolant or not, the liquid cooling systems can be divided into two modes: direct contact and indirect contact. Compared with indirect contact BTMS, the cooling performance of direct contact BTMS is slightly better, but indirect contact BTMS is more suitable for pratical applications [7]. The cooling channel is the most common form of indirect liquid cooling, and the structure of the liquid cooling channel are important factors affecting the performance of indirect liquid cooling BTMS [8]. Many related studies have been conducted to improve the cooling performance of the whole system by optimizing the flow channel and structural design of the liquid-cooled plate [9]. C. Zhao et al. [10] considered a Tesla Model S pack with wavy channels and 71 18650 Li-ion battery modules, showing the thermal characteristics under different charging and discharging conditions. Wang et al. [11] investigated the effect of different cooling structures, a number of microchannel, and inlet mass flow rate on the cooling performance of the system using the maximum temperature and maximum temperature difference as criteria and derived the optimal combination of these factors through orthogonal analysis and comprehensive analysis. The optimization strategies they proposed are very instructive for the design of indirect liquid cooling systems. H. Wang et al. [12] produced a design with 20 18,650 Li-ion batteries and aluminum boards with curved surfaces. The results showed that at 3C discharge rate, the parallel cooling method showed the best thermal characteristics with a maximum temperature of 35.74 °C and a temperature difference of 4.71 °C. H. Zhou et al. [13] proposed a liquid cooling scheme based on a semi-spiral duct considering nine 18650 Li-ion batteries. Changing the flow direction of the fluid was effective in improving the thermal characteristics of the batteries. At a 5C discharge rate, the temperature difference between the maximum temperature at the end of discharge and the battery was 30.5 °C and 4.6 °C. Liang et al. [14] used 20 18650 Li-ion batteries to design a six-cooling channel configuration with a serpentine inner surface and an internal flow channel. By applying a counter flow strategy, more uniform and symmetrical temperatures were achieved at both the battery and module levels, with performance results showing a maximum temperature of 38.95 °C and a maximum temperature deviation of 4.36 °C.

Most existing studies on cooling channels have focused on optimizing the structure, number, flow direction, and flow rate of the flow channels. There has been little discussion on the contact angle between the battery cells and the cooling channels. In real electric vehicles, the contact area of liquid-cooled channels not only influences the thermal performance of the battery pack but also relates to the energy consumption of the BTMS. In this study, four different types of cooling channel structures using liquids (structure A, B, C, and D) with different contact angles for a battery pack are proposed to simulate and investigate their effects on cooling efficiency.

II. MODELING METHOD

2.1. Geometry Models of the Battery pack and Cooling Channel

Usually, power battery packs in electric vehicles are composed of many battery modules. This is convenient for maintenance and replacement. The Li-ion battery studied in this paper is cylindrical battery, the battery model is 18650 which the diameter and height of a single battery are 18 mm and 65 mm, respectively. The battery pack is composed of 72 Li-ion batteries connected in series, the structure is illustrated in Fig.1, the distance between the two cells is 1 mm. This kind of cooling and heat dissipation is a wavy channel which is shown in Fig.2. The contact angles between the battery cells and the cooling channels are θ_1, θ_2 and θ_3. Structure A: $\theta_1 = \theta_2 = \theta_3 = 30^o$, structure B: $\theta_1 = \theta_2 = \theta_3 = 40^o$, structure C: $\theta_1 = \theta_2 = \theta_3 = 50^o$ and structure D: $\theta_1 = 30^o$, $\theta_2 = 40^o$, $\theta_3 = 50^o$.

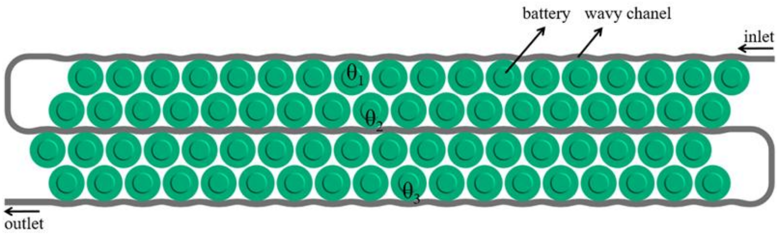

Fig. 1. The geometric model of battery module

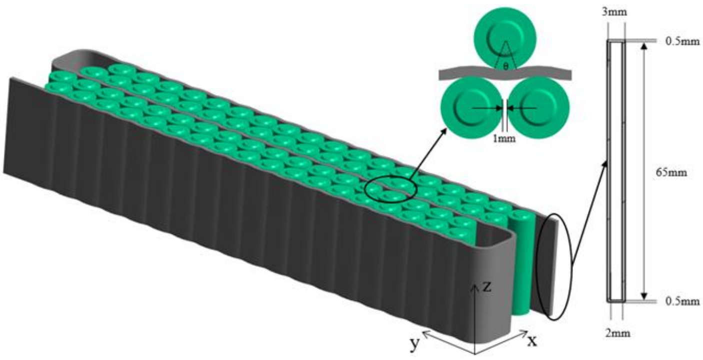

Fig. 2. Geometry parameters of battery module

To carry out numerical simulation, it is necessary to obtain the materials used in each calculation domain. In this study, water with high specific heat and low viscosity is selected as the coolant. Aluminum with low density and good thermal conductivity is chosen as the material for the cooling channel. Due to the layered structure of the battery cell, its thermal conductivity varies greatly in different directions. In this study, anisotropic thermal conductivity is used for the battery cell, the thermal conductivity of the battery cell in each direction is obtained as follows [15]:

$$\lambda_z = 15.8W/(mK); \lambda_x = \lambda_y = 4.52W/(mK)$$

where, the subscripts x, y, and z refer to the directions

Table 1 shows the thermal physical parameters of the materials of the cooling and heat dissipation system of the lithium battery module. Where ρ denotes density, C is heating capacity, λ means thermal conductivity, μ represents dynamic viscosity.

Table 1. Thermal physical parameters of materials for cooling and heat dissipation system [15]

Material	ρ(Kg/m3)	C(J/KgK)	k(W/(mK))	μ(Kg/(ms))
Water	998.2	4128	0.6	$1.003 \times 10{-}3$
Aluminum	2719	891	202.4	-
Battery	1782	1010	15.8	-

2.2 Governing Equations

For the battery, the heat transfer process is controlled by [14]

$$\rho_b C_{p,b} \frac{\partial T}{\partial t} = \frac{\partial}{\partial x}\left(\lambda_x \frac{\partial T}{\partial x}\right) + \frac{\partial}{\partial y}\left(\lambda_y \frac{\partial T}{\partial y}\right) + \frac{\partial}{\partial z}\left(\lambda_z \frac{\partial T}{\partial y}\right) + \dot{Q} \tag{1}$$

where ρ_b denotes the density of battery, kg/m^3; $C_{p,b}$ denotes the constant pressure specific heat capacity of the cell, J/(kg·K); λ_x, λ_y, and λ_z denote the thermal conductivity of the cell domain in the x, y, and z directions, respectively, W/(m·K); $\dot{Q}$ denotes the heat generated by the cell during discharge[15]W/m^3. It is presented as the heat source of the control volume in the calculation.

Liquid water is assumed to be an incompressible fluid. Its continuity equation is expressed as:

$$\frac{\partial v_x}{\partial x}+\frac{\partial v_y}{\partial y}+\frac{\partial v_z}{\partial z}=0 \tag{2}$$

Its momentum equation is shown as:

$$\frac{\partial}{\partial t}\left(\rho_w \vec{v}_w\right)+\nabla.\left(\rho_w \vec{v}_w \vec{v}_w\right)=-\nabla p+\mu_w \nabla^2 \vec{v}_w \tag{3}$$

where $\vec{v}_w$ denotes the velocity vector of the water; where p denotes the static pressure of water, Pa.

Its energy equation is shown in equation:

$$\frac{\partial}{\partial t}\left(\rho_w C_{p,w} T_w\right)+\nabla.\left(\rho_w C_{p,w} T_w \vec{v}_w\right)=\nabla.\left(k_w \nabla T_w\right) \tag{4}$$

where, $C_{p,w}$ is the specific heat capacity of water under constant pressure, J/(kg·K); k_w is the effective thermal conductivity, W/(m·K).

For the wavy channel, the heat transfer process is controlled by the heat transfer differential equation:

$$\rho C_p \frac{\partial T}{\partial t}=\nabla.(k\nabla T) \tag{5}$$

where ρ, C_p, and k denote the density of the corresponding material, kg/m^3, the constant pressure specific heat capacity, J/(kg·K), and the thermal conductivity, W/(m·K), respectively.

2.3 Boundary Conditions

The boundary conditions of the battery at the interface are expressed by the laws of conservation of energy and Newton's law of cooling, as follows:

$$-k_b \frac{\partial T}{\partial n}=-k_f \frac{\partial T}{\partial n} \tag{6}$$

where k_b and k_f are the thermal conductivities of the battery and coolant, respectively. Thermal radiation is neglected. Inlet water temperature was set as 30^{o}C, equal to ambient temperature, and atmospheric pressure was set as the boundary condition at the outlet. The fluid walls, as shown in Fig. 2, are set as a no-slip wall boundary. All the outer walls of the model are set as an insulation boundary, except inlets and outlets. The initial temperature is 30^{o}C. The simulations are performed on the ANSYS FLUENT platform.

III. RESULTS AND DISCUSSION

As all the heat is transferred to the cooling water through the wavy channel, the angle of contact surface between the wavy channel and cell determines whether cooling performance is good or not. In the following study, effects of the contact angle on cooling performance of battery module are discussed in detail.

The cooling efficiency of the four structures in the discharge process at rate of 5 C and the inlet velocity is 0.1 m/s. Fig 3 shows the visualization of the temperature distribution of the 32.5 mm (1/2 battery height) part of the middle height of the battery cell at the end of discharging. The maximum temperature of structure B, structure C and structure D decreased by 1.11 ^{o}C, 1.82 ^{o}C and 1.28 ^{o}C, respectively compared to the structure A. Therefore, the maximum temperature of structure A is the highest, followed by structure B, structure D, and finally, structure C.

IV. CONCLUSIONS

In this study, four different types of cooling channel structures using liquids (structure A, B, C, and D) with different contact angles for 18650 Li-ion battery packs were proposed to simulate and investigate their effects on cooling efficiency under a 5C discharge rate and an inlet velocity of 0.1 m/s. Some conclusions are drawn as follows: (i) The maximum temperature of structure B, structure C and structure D decreased by 1.11 ^{o}C, 1.82 ^{o}C and 1.28 ^{o}C, respectively compared to the structure A; (ii) Structure C had better cooling effect than the other three structures. Further studies will analyze the influence of structural parameters and optimize the cooling channel structure.

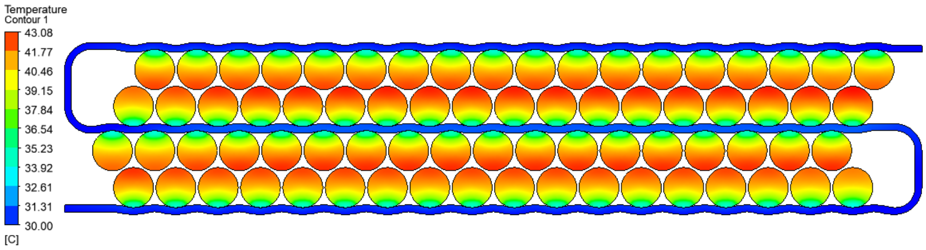

(a) Structure A

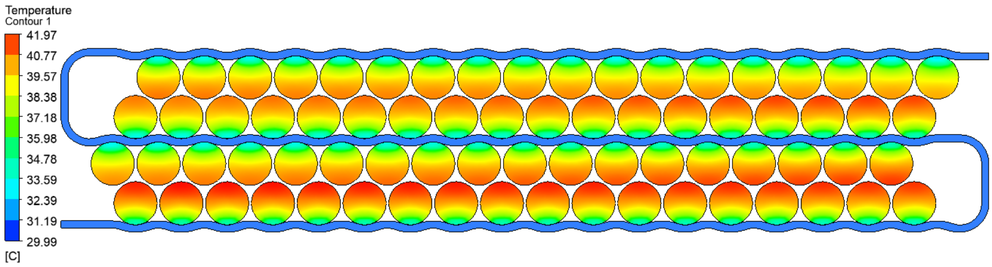

(b) Structure B

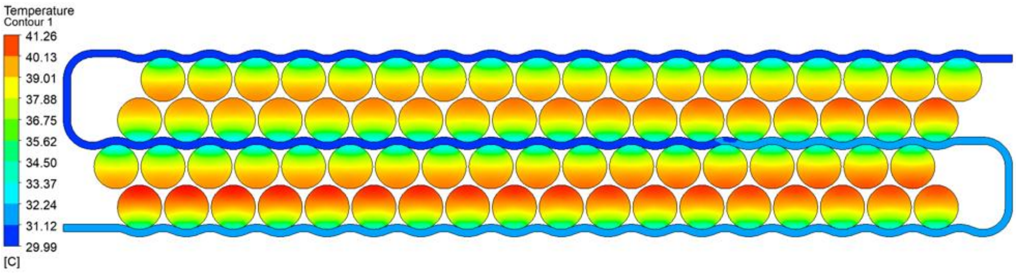

(c) Structure C

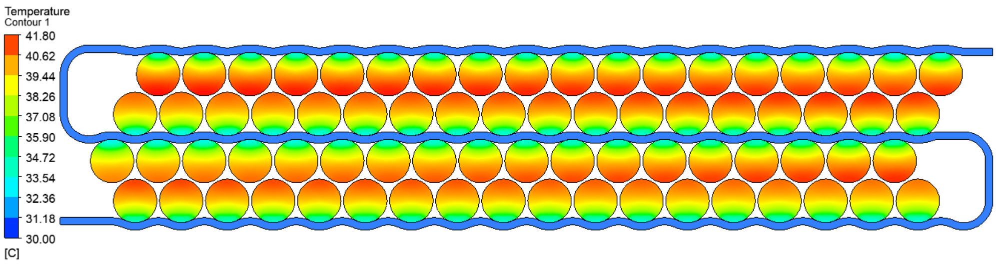

(d) Structure D

Fig 3. Comparisons of temperature distributions of four designs

Acknowledgment

The work described in this paper was supported by Thai Nguyen University of Technology (TNUT) for a scientific project (Code: T2024-NCS11).

REFERENCES

[1] J. Jaguemont, L. Boulon, Y. Dubé, A comprehensive review of lithium-ion batteries used in hybrid and electric vehicles at cold temperatures, Appl. Energy 164 (2016) 99–114.

[2] S. Amjad, S. Neelakrishnan, R. Rudramoorthy, Review of design considerations and technological challenges for successful development and deployment of plug-in hybrid electric vehicles, Renew. Sustain. Energy Rev. 14 (2010) 1104–1110.-Y. Wang et al., ''Lithium-ion battery structure that self-heats at low temperatures,'' Nature, vol. 529, pp. 515–518, Jan. 2016.

[3] A.S. Brouwer, T. Kuramochi, M. van den Broek, A. Faaij, Fulfilling the electricity demand of electric vehicles in the long-term future: an evaluation of centralized and decentralized power supply systems, Appl. Energy 107 (2013) 33–51.

[4] T.M. Bandhauer, S. Garimella, T.F. Fuller, A critical review of thermal issues in lithium-ion batteries, J. Electrochem. Soc. 158 (2011) R1–R25.

[5] Feng X, Fang M, He X, Ouyang M, Lu L, Wang H, et al. Thermal runaway features of large format prismatic lithium-ion battery using extended volume accelerating rate calorimetry. J Power Sources 2014; 255:294–301.

[6] Väyrynen A, Salminen J. Lithium-ion battery production. J Chem Thermodyn 2012; 46:80–5.

[7] D. Chen, J. Jiang, G.-H. Kim, C. Yang, and A. Pesaran, “Comparison of different cooling methods for lithium-ion battery cells,” Applied Thermal Engineering, vol. 94, pp. 846–854, 2016.

[8] J. Wang, S. Lu, Y. Wang, C. Li, and K. Wang, “Effect analysis on thermal behavior enhancement of lithium-ion battery pack with different cooling structures,” Journal of Energy Storage, vol. 32, article 101800, 2020.

[9] W. Zichen and D. Changqing, “A comprehensive review on thermal management systems for power lithium-ion batteries,” Renewable and Sustainable Energy Reviews, vol. 139, article 110685, 2021

[10] Zhao, C.; Cao, W.; Dong, T.; Jiang, F. Thermal behavior study of discharging/charging cylindrical lithium-ion battery module cooled by channeled liquid flow. Int. J. Heat Mass Transf. 2018, 120, 751–762.

[11] J. Wang, S. Lu, Y. Wang, C. Li, and K. Wang, “Effect analysis on thermal behavior enhancement of lithium-ion battery pack with different cooling structures,” Journal of Energy Storage, vol. 32, article 101800, 2020.

[12] Wang, H.; Tao, T.; Xu, J.; Mei, X.; Liu, X.; Gou, P. Cooling capacity of a novel modular liquid-cooled battery thermal man-agement system for cylindrical lithium-ion batteries. Appl. Therm. Eng. 2020, 178, 115591.

[13] Zhou, H.; Zhou, F.; Zhang, Q.; Wang, Q.; Song, Z. Thermal management of cylindrical lithium-ion battery based on a liquid cooling method with half-helical duct. Appl. Therm. Eng. 2019, 162, 114257.

[14] Liang, G.; Li, J.; He, J.; Tian, J.; Chen, X.; Chen, L. Numerical investigation on a unitization-based thermal management for cylindrical lithium-ion batteries. Energy Rep. 2022, 8, 4608–4621.

[15] G. Hao, Reseach on simulation and control of heat transfer characteristics of liquid-cooled battery for pure electric vehicle, China Academic Journal Electronic Publishing House. (2020).